A Preliminary Study on the Experimental Characterization and Modelling of a 20kW Fuel Cell System for Ultralight Aviation

Teresa Donateo[1*], Andrea Graziano Bonatesta[1], Nicolò Franza[1], Antonio Masciullo[1], Roberto Urso[1] and Antonio Ficarella[1]

[1] Department of Engineering for Innovation, University of Salento. Lecce, Italy

[*]E-mail: teresa.donateo@unisalento.it

Abstract. This research is conducted as part of the SERENA project, which aims to develop an electric and modular hydrogen-based powertrain for general aviation. The modular design allows for adaptable power output levels, catering to diverse operational requirements and future scalability. In earlier work, the main powertrain components — the PEM fuel cell, the battery, and the compressed hydrogen cylinder — were dimensioned using a method that prioritizes minimizing both mass and volume. This article details the experimental evaluation of a 20 kW fuel cell module, with particular emphasis on the cathode circuit. It includes a two-stage dynamic compressor, a humidifier, the fuel cell stack, and a backpressure control valve. The testing setup comprises a bi-directional programmable load and a data acquisition system that monitors pressure and temperature throughout the cathode pathway and the compressor's duty cycle. Data collected at sea level were used to calibrate a numerical model that predicts fuel cell performance across flight conditions. As altitude increases, the compressor's parasitic power demand rises, necessitating a corresponding increase in stack current to maintain the target power output. Preliminary findings indicate that raising the flight altitude from sea level up to 2000 meters can cause the compressor's parasitic power to increase by as much as 150% under low-load conditions.

1. Introduction

Phasing out fossil-fuel-powered engines across all types of aircraft is the goal of the air transport sector by 2050, aiming to achieve carbon neutrality [1][2]. Since small piston-engine aircraft constitute a minor portion of overall air traffic, they are overlooked in emissions regulations. However, ultralight aviation has a non-negligible impact on the environment, in particular because of the use of leaded gasoline [3]. Avgas 100LL, the standard fuel for ultralight aviation, emits approximately 3.05 kg of CO_2 per kg of fuel consumed [4] and generates various pollutant emissions due to combustion. Its lead-based anti-knock additive is essential for achieving the necessary octane rating, but is dangerous to people and the environment [5].

To address aviation's environmental challenges, battery-powered propulsion systems have been proposed for small Unmanned Aerial Vehicles (UAVs) and short-range light vehicles for Urban Air Mobility. For heavier applications, the limited specific energy of today's battery technology is insufficient to guarantee the desired flight duration.

Hydrogen presents a promising alternative that could reduce aviation emissions while offering longer flight times than battery-electric systems [6]. It can either replace kerosene in turbine engines or serve as fuel for fuel cells. Among the various types of fuel cells, Proton Exchange Membrane Fuel Cells (PEMFCs) are the most used in transportation due to their relatively higher specific power and efficiency than other fuel cell technologies. Unlike hydrogen combustion, which still produces nitrogen oxides, PEMFCs are quiet, vibration-free, and emission-free devices [7][8].

PEMFCs have been considered for a large variety of aircraft, ranging from small UAVs to commercial airliners, while the application to ultralight aviation is, to the authors' knowledge, limited to the projects listed in Table 1. In all cases, fuel cells are integrated with batteries in hybrid-electric configurations to combine the advantages of both. Fuel cells have a lower power density than modern lithium-based batteries. On the other hand, compressed hydrogen provides a much higher energy density than any existing battery technology.

Table 1. Relevant projects in ultralight aviation

Aircraft	Project	Max Take-Off Weight	FC Power	Source
Motor glider	Boeing Phantom	770 kg	20 kW	[10]
Ultralight	ENFICA-FC	554 kg	20 kW	[11]
Ultralight	Sigma-4	650 kg	35 kW	[12]
Motor glider	Antares DLR-H2	825 kg	3 × 10 kW	[13]
4 pax	H2fly Pipistrel HY4 2016	1500 kg	4 × 10 kW	[16]

In aerospace applications, open-cathode air-cooled fuel cells are adopted for power outputs below 6 kW [10]. For higher powers, liquid-cooled PEM fuel cells are typically employed, as seen in research initiatives such as ENFICA-FC [11] and the Sigma-4 ultralight aircraft [14]. Nevertheless, some studies have explored the potential to extend the operating range of air-cooled fuel cells up to 10 kW, as demonstrated by the Antares [13] and H2fly projects [16]. Air cooling offers advantages such as reduced system complexity and component count.

In the Antares DLR-H2 and H2fly Pipistrel HY4 2016, modular architectures are considered to extend the field of application of air-cooling technology. The adoption of modular configurations for liquid-cooled PEMFCs has been proposed in other fields of applications, mainly residential or industrial, to exceed the size of commercially available single-stack fuel cell systems (SFCS) [14][15]. The modular architecture can be obtained by combining individual SFCS units, each with its dedicated balance of plant, or by designing a multi-stack PEM fuel cell system (MFCS), in which two or more low-power PEMFC stacks are integrated through a shared balance of plant (i.e., fluidic, electrical, and thermal subsystems). In this project, the modularity is chosen to allow the application of the proposed power system to different sizes of aircraft, so the MFCS option is not considered at the moment.

Few details are given in the projects of Table 1 about the sizing of the fuel cell, but apparently it is performed without taking into account the loss of fuel cell performance with altitude [17]. As the aircraft gains altitude, ambient pressure, temperature, and air density all decrease. These changes affect the operating point of the air compressor, altering both airflow and pressure.

Additionally, during sudden increases in power demand, the rate of electrochemical reactions within the fuel cell accelerates, resulting in a spike in hydrogen consumption. However, due to the response delay of the compressor and its motor, there may be an insufficient supply of oxygen to the cathode. This oxygen shortage prevents some of the protons migrating from the anode from participating in the oxygen reduction reaction, thereby impacting fuel cell efficiency and performance. Therefore, optimizing the operation of the compressor under variable load and altitude conditions is a critical issue in the application to ultralight aviation. Even more details can be found about the actual performances of the proposed power train at seal level and in flight.

To fill these gaps, this investigation describes the setup developed to characterize a 20 kW fuel cell, with a particular focus on the air circuit, which is intended for use in a hybrid electric configuration. It proposes a simulation model to estimate the performance of the air circuit under variable flight altitudes.

2. The SERENA project

The SERENA project aims to develop a fully electric, modular powertrain for the Novotech Seagull by integrating battery systems with hydrogen fuel cell technology. The modular approach enables scalable propulsion solutions across a range of power requirements, providing flexibility for various operational scenarios and future upgrades.

The partners of the University of Salento in the SERENA project are the Aerospace Technological District (DTA-Scarl), EnginSoft S.p.A., and Novotec S.R.L..

The project's core activities are:

I. Developing a modular hybrid-electric hydrogen-based powertrain.
II. Estimating its environmental impact with a well-to-wheel approach.
III. Designing, assembling, verifying, and validating a scaled-down demonstrator.
IV. Performing bench tests on the demonstrator.
V. Creating a digital twin of the full-size powertrain.
VI. Virtually integrating the hydrogen-based power system into the reference vehicle to verify feasibility and performance.
VII. Defining safety and certification issues related to the use of compressed hydrogen.

This investigation focuses on the test and analysis of the scale-down demonstrator based on the design of the power system performed in a previous study [18].

2.1 Aircraft, reference mission, and power system

The reference vehicle for the project is the Seagull, a two-seat, high-wing amphibious aircraft featuring a piston-driven propeller configuration. The main specifications of the aircraft and its propulsion system in the original setup are reported in Figure 1.

The simplified scheme of the proposed power system is depicted in Figure 2. The sizing of the elements of the power system, shown in Table 2, was performed with an optimization procedure described in [18], based on the requirements of a typical mission with a maximum flight altitude of 1800 m.

Wingspan	10.5 m
Wing area	13.5 m²
Max gross weight	700 kg
Power loading	6.5 kg/HP

Figure 1. Picture and main specifications of the Novotech Seagull.

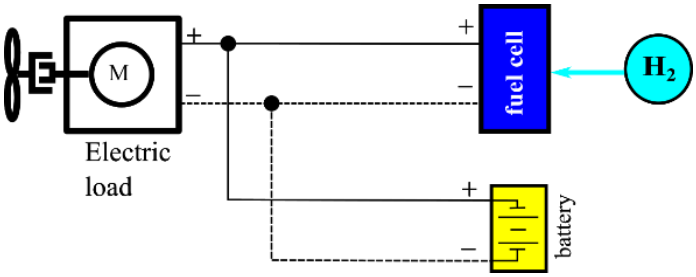

Figure 2. The hydrogen power system

Table 2. Size of the main components of the new power system

	Without onboard Battery Charge	With full On-Board Charging
FC size (kW)	32.5	35.7
Battery size (kWh)	5.9	5
Volume (L) at 700 bar of the H_2 cylinder	57.4	65.4

A comparison of the original gasoline-based powertrain and the power system of **Figure 2** was performed in [19]. In terms of direct emissions, the new powertrain saves approximately 22 kg of CO_{22}, 1.12 g of HC, 15 g of CO, 87 g of NO_x, and 5.3 g of particulate matter in a 90-minute flight and eliminates lead emissions. In terms of well-to-wing emissions, the new powertrain saves up to 266 grams of CO_2 per minute of flight in the case of green hydrogen obtained by using wind energy. With gray hydrogen, the CO_2 saving is only 56 g per minute, and the total emissions of VOCs are much higher than the gasoline-fueled configuration. Details on how these emissions were estimated are reported in [19].

Implementing a hybrid-electric configuration enhances operational safety, as the battery can serve as a backup power source in the event of fuel cell failure. This feature is especially crucial in ultralight aviation, where single-engine propeller systems are common and engine failures often result in fatal accidents [20]. However, the use of hydrogen introduces other safety challenges that require careful design and control of the entire hydrogen system [21]. These aspects are being addressed within the SERENA project and will be further explored in future studies by the project partners.

Based on the results obtained in the previous study [18] and other similar projects (Table 1), it was decided to design a modular system with two SFCSs, each with a maximum power of 20 kW.

Effect of altitude

The net power and efficiency of a liquid-cooled closed-cathode FC are strongly affected by the parasitic power of the compressor, which can be calculated as:

$$P_{comp} = G_{air} c_p T_a(z) \cdot \frac{\left[\left(\frac{p_c}{p_a(z)}\right)^{\frac{k-1}{k}} - 1\right]}{\eta_c} \quad (1)$$

In this equation, $T_a(z)$ and $p_a(z)$ represent the atmospheric temperature and pressure at altitude z, respectively. G_{air}denotes the mass flow rate of air sent by the compressor to the cathode, while c_p and k are the constant pressure specific heat and the specific heat ratio of the air, respectively. The compressor efficiency η_c is inclusive of the electric motor's efficiency.

The mass flow rate G_{air} is mainly dependent on the stack current I_{stack} [22]:

$$G_{air} = 3.57 \cdot 10^{-7} \cdot \lambda_{air} \cdot I_{stack} \cdot N_c \quad (2)$$

Where N_c and λ_{air} are the number of cells in series and the stoichiometric ratio, respectively.

The International Standard Atmosphere (ISA) model is used to establish the values of temperature and pressure at altitude z (expressed in meters):

$$T_{amb}(z) = T_0 - 6.5\, z \quad (3)$$

$$p_{amb}(\mathrm{z}) = p_0 \left(1 - 6.5 \frac{\mathrm{z}}{T_0}\right)^{5.2561} \quad (4)$$

With $T_0 = 288.15$ K and $p_0 = 101.3$ kPa

The ambient conditions are then used to calculate the corrected mass flow rate as follows:

$$G_{corr} = G_{air} \frac{p_0}{p(z)} \sqrt{\frac{T_{amb}(z)}{T_0}} \quad (5)$$

The proposed fuel cell system is operated at constant cathode pressure p_c by controlling the compressor speed. The stack temperature is controlled by the liquid cooling system. Therefore, the effect of altitude on the polarization curve can be overlooked [9][22]. However, the increase in altitude results in a higher parasitic power because the compressor pressure ratio is higher. Therefore, an increase in the stack current is required to match the desired value of net output power $P_{fc}(i, z)$.

The effects described above are shown, qualitatively, in Figure 3. Where the increases from 0 m to 2000 m., the corrected mass flow rate gets bigger because the increase in $\frac{p_0}{p(z)}$ is not compensated by the decrease of $\sqrt{\frac{T_{amb}(z)}{T_0}}$ in Equation (3). For this reason, the compressor's operating point shifts toward lower flow rates in Figure 3a.

To overcome the increased parasitic power with the same net power, the stack current increases, resulting in a reduction in voltage (Figure 3a). Therefore, increasing altitude reduces overall efficiency because of two combined effects:

- The reduction of the net efficiency of the stack, defined as $\eta_V = \frac{V_{st}}{N_S 1.25}$ [22], due to the increased stack current.
- The increase in the power absorbed by the compressor.

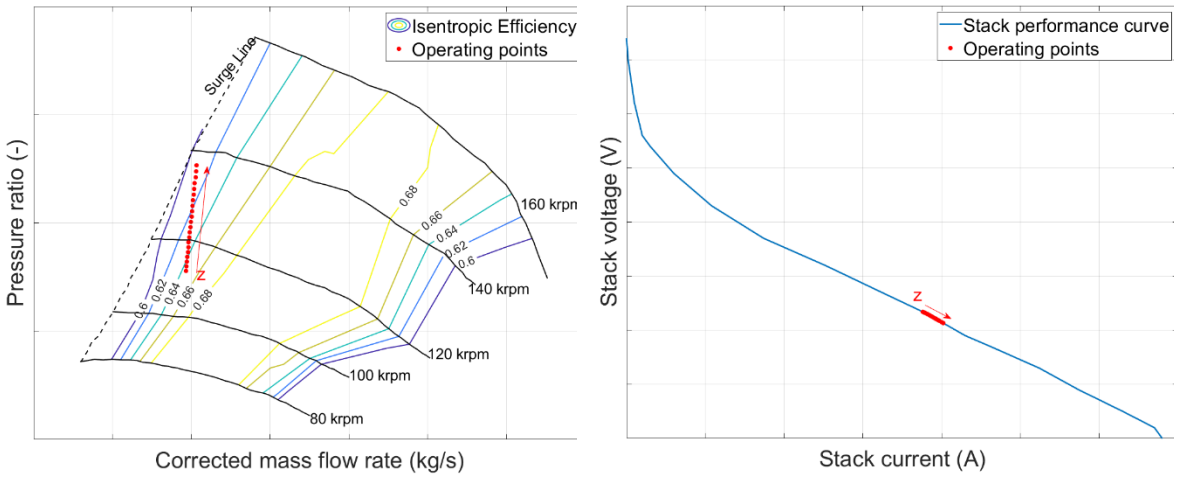

(**a**) (**b**)

Figure 3. Effect of increasing altitude from sea level up to 2000 m on the operating points of the fuel cells system (red circles) shown on (**a**) the performance map of the compressor, (**b**) the polarization curve

The fuel cell system and the experimental setup

The acquired fuel cell is shown in Figure 4 (left), while its main specifications are reported in Table 3. It is a liquid-cooled PEM fuel cell with hydrogen recirculation as shown in the flow chart of Figure 5. To test the system with the typical load request of a flight, we acquired a bidirectional electronic load consisting of two modules with a nominal power of 18 kW (see Figure 4, right, and Table 3).

Figure 4. Pictures of the experimental setup showing the fuel cell system (left) and the bidirectional electronic load (right)

Table 3. Specification of the fuel cell and the bidirectional electronic load

Fuel cell	Nominal voltage	144 volt
	Maximum power	20 kW
	Number of cells	
	Efficiency at maximum power	45 %
	Operating temperature	-20 / +50°C
	Cooling	Liquid
	Max hydrogen pressure (relative)	1 bar
	Communication protocol	Can Bus
Bidirectional load	Minimum efficiency	95%
	Max voltage	≥ 300V
	Max current	≥ +/- 400A
	Max power	≥ +/- 36kW
	Minimum voltage	1,8V
	Load signal	CC/CV/CP/CR
	Communication	USB-TMC or VCP /LAN/CAN/Digital I/O

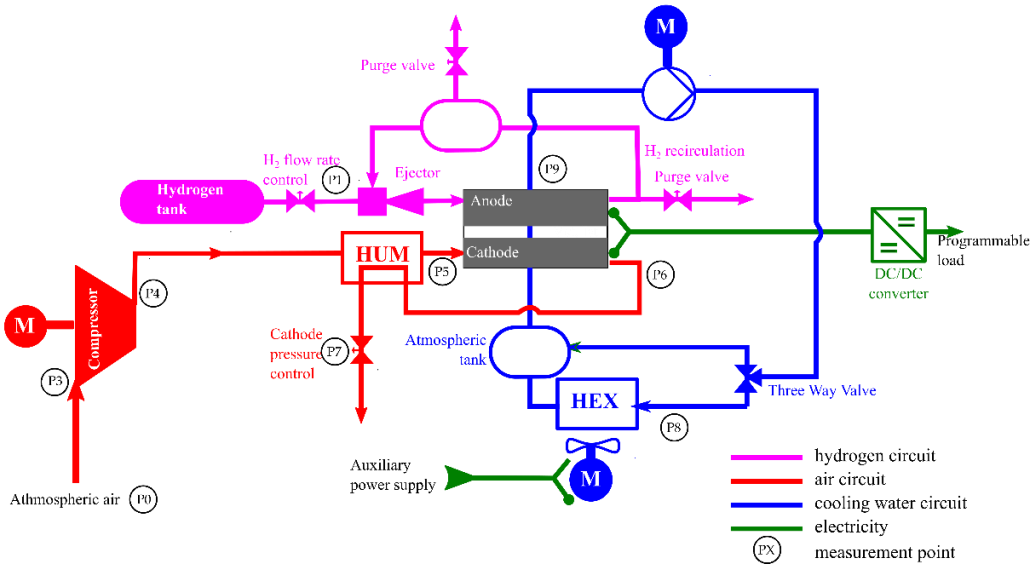

Figure 5. Flowchart of the balance of plant and position of the measurement points

The setup of the fuel cell was designed for research purposes, so it is equipped with several sensors for pressure, temperature, flow rate, and other parameters, and features open access to allow for modification to both the hardware and software utilities. For the same reason, the compressor and the other auxiliaries are powered by a separate supply.
The primary measurement points in the fuel cell systems are also displayed in Figure 5. Thanks to the modularity and bidirectionality of the programmable electronic load, it is possible to perform various tests for characterizing the hybrid electric power system, as illustrated in Figure 6. The two modules can be used to characterize fuel cell systems (Figure 6a) or battery packs (Figure 6b) separately, up to 36 kW. They can be used together to test the whole powertrain, including the electric motor. Finally, the emulator can be used to simulate the battery alone, as shown in Figure 6c and Figure 6d.

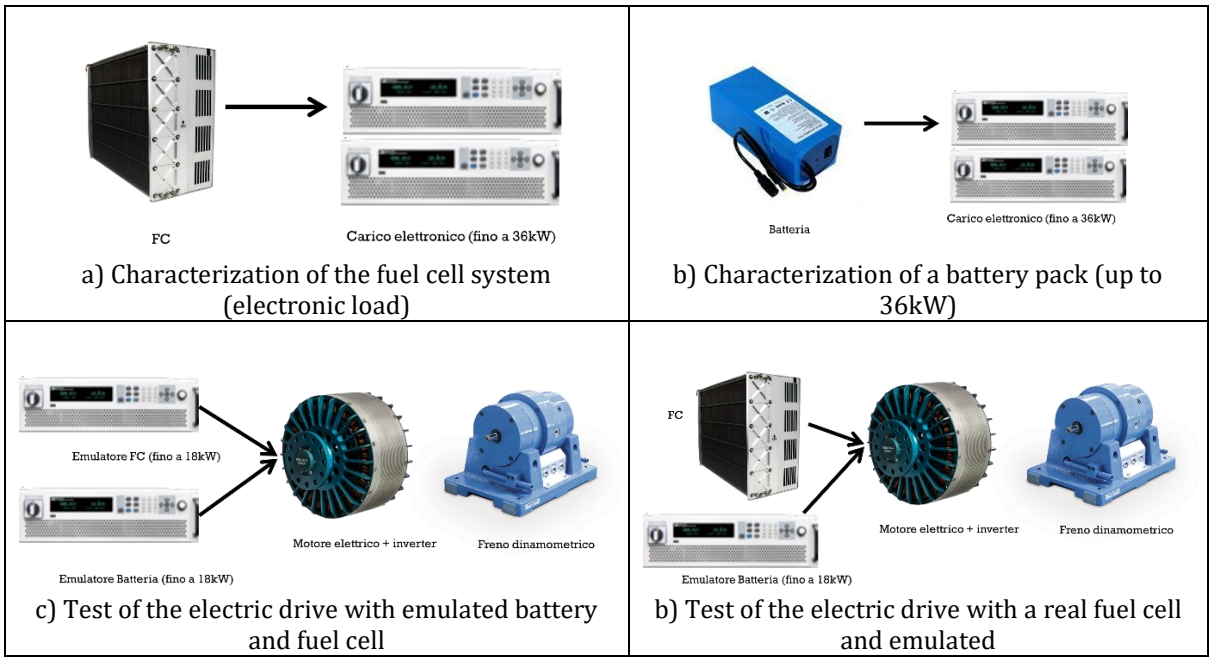

a) Characterization of the fuel cell system (electronic load)

b) Characterization of a battery pack (up to 36kW)

c) Test of the electric drive with emulated battery and fuel cell

b) Test of the electric drive with a real fuel cell and emulated

Figure 6. Possible testing scenarios with the modular bidirectional electronic load

3. Dynamic modeling of the air circuit

To estimate the effect of altitude on the performance of the air circuit and, in the future, optimize the compressor performance, the authors implemented the model depicted in Figure 7.

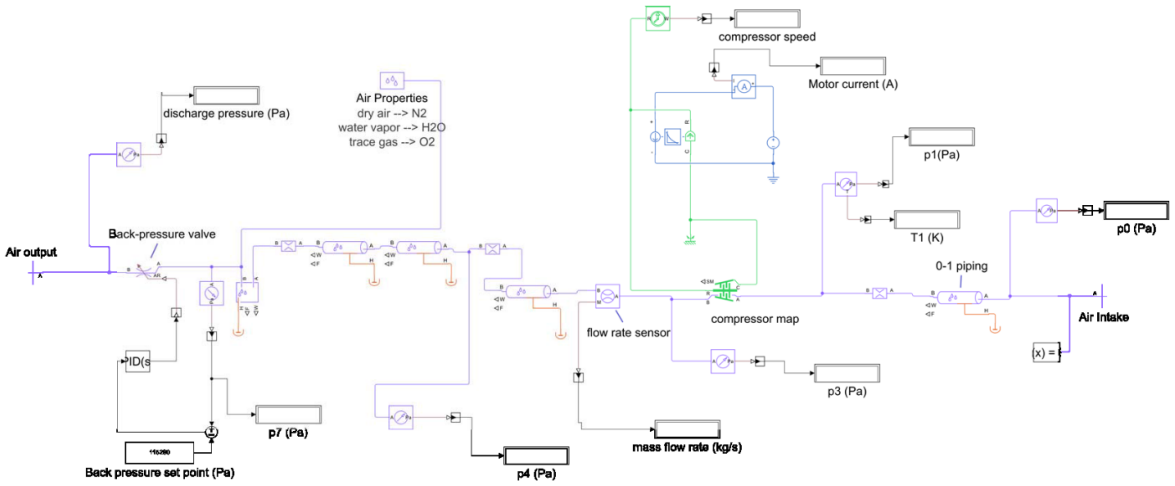

Figure 7. Model of the air circuit implemented in MATLAB/SimScape

4. Preliminary results

A preliminary analysis of the fuel cell was conducted using the set points listed in Table 4.

Table 4. Setpoints and main measured parameters for the stack tests (ambient conditions 15°C, 99kPa, RH 67%)

	A	**B**	**C**	**D**
Flight phase	Descent	Cruise	Climb	Takeoff/Climb
Current set point (A)	27	103	150	155
Power (kW)	3	11.1	14.7	15.3
Voltage (V)	118.3	106.4	95.1	99.4

These data show a typical reduction of voltage with current, which also determines the reduction of voltaic efficiency of the stack from 66% to 53%. Note that the measurement of the hydrogen mass flow rate is not yet available, as the setup is still in progress; therefore, the global efficiency of the system cannot be evaluated yet.

The first setpoint represents the minimum power at which the fuel cell is allowed to operate, while Setpoint B roughly corresponds to the maximum efficiency point declared by the manufacturer. A further increase in current leads to the generation of a higher stack power at the expense of efficiency. The setpoints C and D correspond to compromise operating points between the two performance indexes. The four setpoints qualitatively represent the typical power distribution in the main segments of the flight, as reported also in Table 4.

The plot of Figure 8 shows the pressure values along the air circuit (regarding the measurement points of Figure 5). Notice that the control of the backpressure opening defines a constant pressure at measurement point P7. The pressure, after being increased in the compressor, decays due to pressure losses in the humidifier and, above all, in the stack. It is essential to note that, unlike what is typically assumed for a closed-cathode fuel cell, the stack pressure is not constant but increases with the load. Therefore, the stack efficiency is affected by the compressor control strategy.

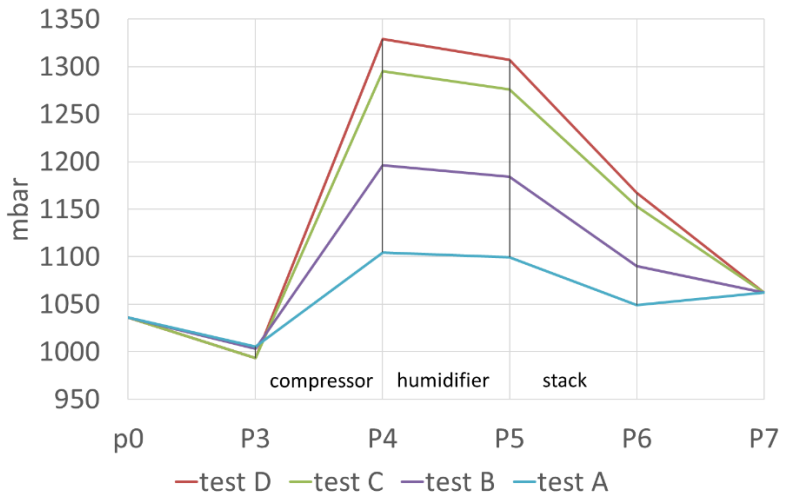

Figure 8. Pressure variation along the test points of the cathode line

Table 5. Compressor operating points

	A	**B**	**C**	**D**
Current set point (A)	27	103	150	155
Air flow (Nm3/h)	16.6	27.5	38.6	39.5
Pressure ratio	1.10	1.19	1.30	1.34
λ_{st}	4.1	1.8	1.7	1.7

The details of the compressor operating points are reported in Table 5. The value of λ_{st} guaranteed by the compressor was found to be about 1.7 for all tests except for test #A, where it was 4.1. This parameter is typically maintained between 1.5 and 2.0 [11][22] as a compromise between the positive effect on stack efficiency obtained with increasing air flow and the negative effect of increased parasitic power. The results reported in Table 5 indicate that the compressor is not optimized for operation at low load. The parasitic power is significantly higher than in the case of setpoint D, where it is 9% of the stack power.

The data acquired in the preliminary tests were used to characterize the components of the air circuit shown in Figure 7 and to estimate the parasitic power of the compressor on the current setpoints of Figure 5 when the altitude is increased up to 2000m. Please note that the details of the compressor map are now reported here due to a confidentiality agreement.

From the results of Figure 9, we can notice that the effect of altitude is more relevant at low load (Test A). In this case, the increase in altitude from sea level to 2000m more than doubles the compressor parasitic power (+150%), while at the higher load (Test D), the increase is relatively lower (+61%).

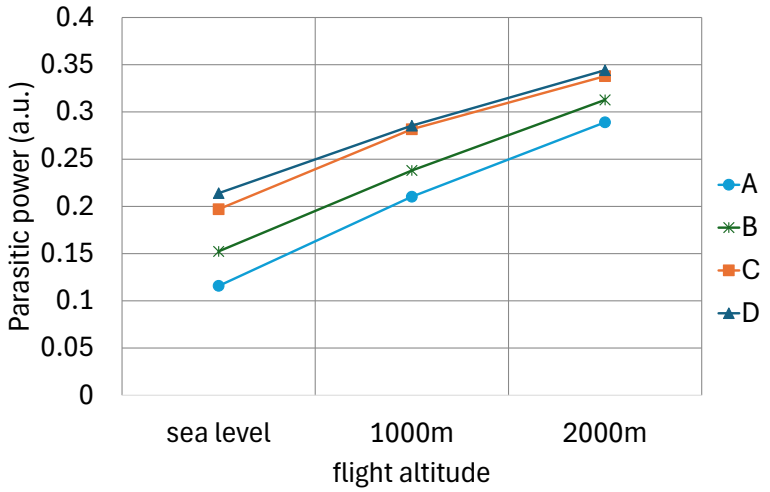

Figure 9. Parasitic power of the compressor vs altitude at the four setpoints

Conclusions and future work

After describing the sizing procedure adopted by the authors to design a hybrid electric powertrain with a fuel cell for ultralight aviation, this paper presents the modular experimental setup acquired for testing the fuel cell system under variable load values typical of the specific application.

Thanks to the modularity and bidirectionality of the programmable electronic load, it is possible to perform various tests for characterizing the hybrid electric power system. The two modules can be used to characterize fuel cell systems or battery packs separately. They can be used together to test the entire powertrain, including the electric motor, with the battery or fuel cell replaced by one of the modules used as an emulator.

The preliminary results of stationary tests performed at four load levels (approximately 3kW to 15kW) were presented and discussed. The modeling of the cathode line of the fuel cell system in MATLAB/Simscape language was used to predict the effect of height above sea level on the parasitic power of the cathode line, a critical aspect in the application to the aerospace field.

Future activities will focus on the comprehensive characterization of fuel cell systems and the thorough validation of the proposed model at sea level. Moreover, the emulator capability of the programmable load will be utilized to study the coupling of the fuel cell with various lithium battery technologies.

Acknowledgments

This investigation is part of the project “Sviluppo di architetture propulsive ad emissioni zero per l’Aviazione generale (SERENA—CUP: F89J22003510004),” funded by the Italian Ministry for the Environment and Energy Security (MASE), M2-C2-I3.5 call of the Italian Recovery and Resilience Plan. The authors would like to thank the other project partners (Novotech, DTA-Scarl, and EngineSoft s.p.a.) for their valuable suggestions and helpful support.

References

[1] The ATI FlyZero team 2022. *Available online*: https://www.ati.org.uk/ (accessed on 2 January 2024).

[2] The Clean Sky 2 team 2020 https://doi.org/10.2843/471510. Available online: https://www.euractiv.com/wp-content/uploads/sites/2/2020/06/20200507_Hydrogen-Powered-Aviation-report_FINAL-web-ID-8706035.pdf (accessed on 2 January 2024).
[3] Rizvi S A Q, Kearns S, Cao S, 2024 *Air* **2**, 162–177 https://doi.org/10.3390/air2020010.
[4] Kumar T, Mohsin R, Ghafir M F A, Kumar I, Wash A M 2018 *Chem. Eng. Trans* **63** 181–186.
[5] Mills A, Peckham S 2022 *Public Health Chall.* 1 e27.
[6] Abdelkareem M A, Elsaid K, Wilberforce T, Kamil M, Sayed ET, Olabi, A. 2021 *Sci. Total Environ.* **752**, 141803.
[7] Baroutaji A, Wilberforce T, Ramadan M, Olabi A G 2019 *Renew. Sustain. Energy Rev.* **106** 31–40. https://doi.org/10.1016/j.rser.2019.02.022.
[8] Granovskii M, Dincer I, Rosen M A 2006 *J. Power Sources* **157** 411–421 https://doi.org/10.1016/j.jpowsour.2005.07.044.
[9] Donateo T 2023 *Energies* **16**, 7676. https://doi.org/10.3390/en16227676.
[10] Lapeña-Rey N, Mosquera J, Bataller E, Ortí F 2007 *SAE Technical Paper* No. **2007-01-3906** https://doi.org/10.4271/2007-01-3906.
[11] Romeo G, Cestino E, Correa G, Borello F 2011 *SAE Int. J. Aerosp.* **4** 724–737 https://doi.org/10.4271/2011-01-2522.
[12] Geliev A V, Varyukhin A N, Zakharchenko V S, Kiselev I O, Zhuravlev D I 2019 *International Conference on Electrotechnical Complexes and Systems (ICOECS)* Ufa Russia 21–25 October 2019 pp. 1–17 https://doi.org/10.1109/ICOECS46375.2019.8949950.
[13] Rathke P, Thalau O, Kallo J, Schirmer J, Stephan T 2013 *Proceedings of the Deutscher Luft- und Raumfahrtkongress* Stuttgart, Germany 10–12 September 2013 p. 301219.
[14] Marx N, Boulon L, Gustin F, Hissel D, Agbossou K. 2014 *Int J Hydrogen Energy* **39**(23) 12101–11.
[15] Abuzant S, Jemei S, Hissel D, Boulon L, Agbousso K, Gustin F. 2017 *Ieee Vehicle Power and Propulsion Conference (Vppc)* 1–6.
[16] Gao Y, Jausseme C, Huang Z Yang T 2022 *IEEE Electrif.* **10** 17–26. https://doi.org/10.1109/MELE.2022.3165725.
[17] Zhao D, Xia L, Dang H, Wu Z, Li H 2022 *Energy Convers. Manag.* **253** 115159 https://doi.org/10.1016/j.enconman.2021.115159.
[18] Donateo T, Ficarella A, Lecce L 2024 *European Transport Studies* **1** 100002.
[19] Donateo T, Bonatesta A G, Ficarella A, Lecce L 2024 *Energies* **17** (13), 3272.
[20] Donateo T, Spada Chiodo L 2023 *Applied Sciences* **13**(7) 4155.
[21] Tveitan S 2020 Life Cycle Assessment of Hydrogen Fuel in Aviation *Master's Thesis* University of Bergen Norway
[22] Larminie J, Dicks A, McDonald M.S. 2003 *Fuel Cell Systems Explained* (Chichester: Wiley)